Available at
www.ElsevierMathematics.com
POWERED BY SCIENCE DIRECT®

APPLIED MATHEMATICS AND COMPUTATION

ELSEVIER Applied Mathematics and Computation 148 (2004) 809–821
www.elsevier.com/locate/amc

Dusty gas model of flow through naturally occurring porous media

Fathi M. Allan [a,*], Naji Qatanani [b], Imad Barghouthi [c], Khaled M. Takatka [b]

[a] *Department of Mathematics, Birzeit University, P.O. Box 14, Birzeit, Palestine*
[b] *Department of Mathematics, Al Quds University, Abu Deis, Jerusalem, Palestine*
[c] *Department of Physics, Al Quds University, Abu Deis, Jerusalem, Palestine*

Abstract

In this article, we develop a set of partial differential equations describing the flow of a dusty fluid in variable porosity media. The developed equations take into account the effect of the porous microstructure on the flowing phases.

We presented and overview of the equations governing the flow of a dusty gas in various type media, including that in naturally occurring porous media. Numerical techniques are used to solve the set of partial differential equations describing the flow for different values of the porous media parameters of interest. These parameters are the Forchheimr drag coefficient C_d, the permeability η and the Reynold number Re.

1. Introduction

Gas-particle flow, dusty fluid flow and the flow of suspension through porous media have received considerable attention due to the importance of these types of flow in studies associated with the design of industrial filters, liquid-dust seperators and water purification plants.

* Corresponding author. Current address: Department of Mechanical Engineering MIT, 77 Mass. Ave. 3-339, Cambridge, MA 02139, USA.

E-mail addresses: fathi@mit.edu, fathi@birzeit.edu (F.M. Allan), naqatanani@yahoo.com (N. Qatanani), barghouthi2@yahoo.com (I. Barghouthi).

0096-3003/$ - see front matter
doi:10.1016/S0096-3003(02)00939-6

Applications of the above types of flow in the environment are exhibited in solid-waste and pollutant dispersal and storage in the ground layers. Fluid flow through porous media has become a topic of increasing importance due to its applicability in many physical situation including the prediction of oil reservoir behavior, ground water flow, irrigation problems and the biophysical sciences where the human lungs for example, are modeled as porous layers.

The above and many other applications emphasize two fundamental aspects of the study of gas particulate flow in porous media

(i) Models describing gas–particulate flow through porous media must accurately take into account the effect of the porous media quantities on the flow constitute on each other, this necessitates developing model that take into account the porous microstructure and its effects on the flowing phases.
(ii) Solution of boundary and initial value flow problems that should accurately predict the flow patterns and the nature of the flow fields of the constituents involved.

A model describing the flow of a dusty gas in porous media was developed in [5] and it is based on the differential equations approach. It incorporates the factors affecting the gas–particulate mixture in the type of porous media where Brinkman's equation is applicable and thus inertial effects were ignored under the assumption of creeping motion in a high-porosity medium.

Dusty fluid flow through porous media with applications to deep filtration has been widely studied in [7] via the empirical and semi-empirical approach, the suggested model takes into account the optimal design of filters, liquid-dust separation and clogging mechanisms of the pores. In the case of flow of suspensions through a deep porous bed the authors in [7] gave a review of the a available literature and outlined the mechanisms of deposition and the possible capturing processes which include sedimentation, inertial impacting, direct interception, hydrodynamic effects and diffusion by Brownian motion.

In cases where the particle size is greater than 1 μm, the particle diffusion is negligible [6] while the effect of inertial impacting is negligible if the fluid-phase is liquid [9]. In additional, if the particles are spherical in shape then the hydrodynamic effects can be neglected [7]. This leaves the interception capture mechanism to be dominant and the particles are captured mainly on the surfaces of the media grains. Settling of particles by sedimentation is also possible due to the high density associated with the dust particles.

Equations governing flow of a dusty fluid between two porous flat plates with suction and injection are developed and closed-form solutions for the velocity profiles, displacement thickness and skin friction coefficients for both phases are obtained. Graphical results of the exact solutions are presented and discussed [1].

The problem of gas-particulate flow through a two-dimensional porous channel bounded by curved boundaries is considered [6], and a set of general averaged transport equations for a multi-phase system consisting of an arbitrary number of phased, interfaces and contact lines is established in [8]. A structure for the system is proposed and hydrodynamic interaction between the phases, interfaces and contact lines is also presented.

2. Mathematical formulation

The steady flow of an incompressible dusty fluid in a porous medium of constant permeability is given by the following coupled set of equations. These equations take into account the absence of dust effects, that is, the fluid-phase momentum equation takes the well-known Darcy–Lapwood–Brinkman (DLB) form. In this type of porous media the speed of the flow is not small and the viscous shearing action is important [4,8]. The set of equations are:

The fluid-phase equations given by

The continuity equation

$$\nabla \mathbf{u} = 0 \tag{1}$$

and the momentum equation

$$\rho \mathbf{u} \nabla \mathbf{u} = -\nabla p + \mu \nabla^2 \mathbf{u} - \frac{\mu}{\eta} \mathbf{u} \tag{2}$$

The dust-phase equations given by

The continuity equation

$$\nabla . N \mathbf{v} = 0 \tag{3}$$

and the momentum equation

$$\mathbf{v} \nabla \mathbf{v} = k/m(\mathbf{u} - \mathbf{v}) \tag{4}$$

where $\mathbf{u}$ and $\mathbf{v}$ are the fluid and dust macroscopic velocity vectors, p is the pressure, μ is the viscosity coefficient, ρ is the density, N is the particle number density, m is the mass of a single dust particle, η is the permeability and k is the drag coefficient on the dust particle in the porous medium.

The fluid-phase momentum equation (2) is valid in a variety of settings and in different types of porous media. We will discuss the following cases that illustrate the variety of settings and the different types that this equations is valid in [3,6–9].

(i) When the inertial effects are negligible or insignificant, that is, the flow is fully developed with no macroscopic stream-wise fluid-phase velocity gradient, Eq. (2) becomes

$$-\nabla p + \mu\nabla^2\mathbf{u} - \frac{\mu}{\eta}\mathbf{u} = 0 \tag{5}$$

Eq. (5) is known as Brinkman's equation which is postulated to be valid in situations where the porosity of the medium is close to unity.

(ii) When the macroscopic boundary effects are not important, that is when the macroscopic cross-stream fluid-phase velocity gradients are absent, Eq. (2) yields

$$\rho\mathbf{u}\nabla\mathbf{u} = -\nabla p - \frac{\mu}{\eta}\mathbf{u} \tag{6}$$

Eq. (6) is known as Darcy–Lapwood (DL) model and it is valid when the porous medium possesses a sparse structure that is the flow is through a sparse distribution of particles fixed in space.

(iii) When the inertial effects and viscous shearing effects are neglected, that is, both of the macroscopic stream-wise and cross-stream fluid-phase velocity gradients are absent, Eq. (2) yields

$$-\nabla p - \frac{\mu}{\eta}\mathbf{u} = 0 \tag{7}$$

Eq. (7) is Darcy's law which describes the motion of a single-phase fluid flow through porous media.

(iv) When the porous medium is naturally occurring, the fluid-phase momentum equation reduces to a Forchheimer's equation that is postulated to govern the single-phase fluid flow, the resistance to the fluid offered by the porous matrix is governed by an equation of the form.

$$-\nabla p = \alpha\mathbf{u} + \beta\mathbf{u}|\mathbf{u}| \tag{8}$$

where $\alpha = \mu/\rho\eta$, $\beta = C_d/\sqrt{\eta}$, and C_d is the Forchheimer drag coefficient and β is referred to as the inertial parameter.

The dust-phase momentum equation (4) serves in all of the different types of porous media which take the above discussed cases so the macroscopic cross-stream velocity gradients are absent while the stream-wise velocity gradients are always present. In the presence of an impermeable boundary as a solid wall or otherwise, the dust particles settle on the macroscopic boundary and set into motion other particles that are already settled, while others reflect back into the flow field and assume a streamwise velocity gradients. Consequently, the macroscopic convective term $\mathbf{u}\nabla\mathbf{u}$ always survives.

3. Flow through a naturally occurring porous channel

In this section, the two-dimensional flow of an incompressible dusty fluid through naturally occurring porous channel into a point-sink is considered. The source–sink model which is a popular setting for irrigation problems,

might be thought of here as a means for solid-waste disposal. The model at thus shed some light on the behavior of the solid particles in the flow field as they are dispersed in a porous layer. The determinate nature of the model equations is illustrated by numerically studying the flow at hand.

The flow setting under consideration is governed by the coupled set of Eqs. (1), (3), (4) and (8).

We introduce the dimensionless macroscopic streamfunctions $\mathbf{\Psi}_1(x,y)$, and $\mathbf{\Psi}_2(x,y)$ and macroscopic vorticities $\zeta_1(x,y)$ and $\zeta_2(x,y)$ in terms of the dimensionless horizontal and vertical components of velocity defined by

$$u_1 = \mathbf{\Psi}_{1y}, \quad v_1 = -\mathbf{\Psi}_{1x}$$
$$u_2 = \mathbf{\Psi}_{2y}, \quad v_2 = -\mathbf{\Psi}_{2x}$$

And the dimensionless vorticities are defined by

$$\zeta_1 = v_{1x} - u_{1y}$$
$$\zeta_2 = v_{2x} - u_{2y}$$

The stream function vorticity equations governing the flow at hand in each of the coupled set of Eqs. (1) and (8) for the fluid-phase, and Eqs. (3) and (4) for the dust-phase are obtained by taking the curl of each of the momentum equations and the subsequent use of the equations of continuity and are given by the following set of equations [8]:

The fluid-phase equations:

$$\nabla^2 \mathbf{\Psi}_1 = -\zeta_1 \tag{9}$$

and

$$\frac{\zeta_1}{\eta Re}\sqrt{\mathbf{\Psi}_{1x}^2 + \mathbf{\Psi}_{1y}^2} + \frac{\zeta_1 C_\mathrm{d}}{\sqrt{\eta}}\left\{\mathbf{\Psi}_{1x}^2 + \mathbf{\Psi}_{1y}^2\right\} = \frac{C_\mathrm{d}}{\sqrt{\eta}}\left\{\mathbf{\Psi}_{1x}^2\mathbf{\Psi}_{1xx} + 2\mathbf{\Psi}_{1x}\mathbf{\Psi}_{1y}\mathbf{\Psi}_{1xy} + \mathbf{\Psi}_{1y}^2\mathbf{\Psi}_{1yy}\right\} \tag{10}$$

and the dust-phase equations:

$$\nabla^2 \mathbf{\Psi}_2 = -\zeta_2 \tag{11}$$

and

$$\mathbf{\Psi}_{2y}\zeta_{2x} - \mathbf{\Psi}_{2x}\zeta_{2y} = \frac{K}{M}[\zeta_1 - \zeta_2] \tag{12}$$

The flow variables have been rendered dimensionless with respect to a characteristic velocity U_∞ and a characteristic length L using the following dimensionless equations:

$X = x/L,\ Y = y/L,\ \vec{U} = \vec{u}/U_\infty,\ \zeta = \zeta^* L/U_\infty,\ K = k/L^2,\ \mathbf{\Psi} = \mathbf{\Psi}^*/LU_\infty$ and the Reynolds number is defined as $Re = \rho U_\infty L/\mu$.

4. Numerical example

Consider the flow of dusty fluid in a straight porous channel, bounded below and above by impermeable walls. Associated with this flow are boundary conditions and entry conditions to the channel. Any appropriate boundary conditions must be compatible with the type of medium, the governing model equations and the type of the impermeable bounding walls.

Suitable boundary conditions for the flow at hand, in the shown configuration, are as follows:

$\Psi_1 = \Psi_2 = 0$ along the walls ab and bc
$\Psi_1 = \Psi_2 = 1$ along the upper wall dc
$\Psi_1 = \Psi_2 = y$ $0 \leqslant y \leqslant 1$ along the ad

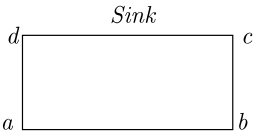

Channel Configuration

The fluid-phase and the dust-phase velocities are quantities to be determined on the impermeable walls. In addition no explicit boundary conditions are available for the vorticities of the phases involved. Thus, ζ_1 and ζ_2 are updated on the boundary in terms of the streamfunction values at internal grid points using standard first-order accurate schemes. On the boundary in terms of the streamfunction values at internal grid points using standard first-order accurate schemes.

Numerical integration is therefore accomplished by solving Eqs. (9) and (10) iteratively using successive over-relaxation techniques.

Results have been obtained for various values of permeability, Forchheimer drag coefficient and Reynolds number. The test cases considered are permeability $k = 1, 0.1, 0.01$ and 0.00001, drag coefficient $C_d = 0.5, 0.55, 0.75$ and for the Reynolds number $Re = 0.5, 0.65, 0.85$ and 1.

Solutions were obtained using a step size $H = \Delta X = \Delta Y = 0.01$ for the computational domain $[0,1] \times [0,1]$. The numerical scheme presented in [2,9] is used for solving Eq. (9) and it is given by

$$\Psi_{(i,j)}^{(n+1)} = \Psi_{(i,j)}^{(n)} + \frac{\omega}{4}\left(\Psi_{(i-1,j)}^{(n+1)} + \Psi_{(i+1,j)}^{(n)} + \Psi_{(i,j-1)}^{(n+1)} + \Psi_{(i,j+1)}^{(n)} - 4\Psi_{(i,j)}^{(n)} - H^2\zeta(i,j)\right) \tag{13}$$

The iterated result converges for $1 \leqslant \omega < 2$, and it converges most rapidly where ω is assigned the optimum value

$$\omega = \frac{4}{2 + \sqrt{4 - \left[\cos\left(\frac{\Pi}{m}\right) + \cos\left(\frac{\Pi}{n}\right)\right]^{-2}}} \tag{14}$$

where *nXm* is the grid dimension. The stream function may take an arbitrary additive constant, in order to start the iteration, a constant value of 0.5 is guessed fore the stream function at all interior points. The absolute value of the difference between this and the previous value of Ψ_1 at the same point is calculated and is added to the value of a variable called ERROR, whose starting value at the beginning of an iteration is zero. At the end of one iteration, when the values of Ψ_1 at all interior points have been updated, the value of ERROR is compared with ERRMAX. If ERROR is less than or equal to ERRMAX, then calculate the value of ZETA 1. Whose starting value at the beginning of iteration is zero, the absolute value of the difference between this and the previous value of ZETA 1. At the same point is calculated and is added to ERROR. At the end of one iteration, when the values of ZETA 1 At all interior points have been reached, so the iterating process can be stopped. Otherwise, the iteration counter ITER is increased by 1 and a new iteration is started. In our program we let $\mathrm{ERRMAX} = 0.1 \times 10^{-5}$.

After convergence, the fluid and dust velocity components are calculated in terms of Ψ_1 by backward difference schemes. The fluid-phase vorticity is then calculated using a finite difference form of Eq. (9). The same techniques is applied to the coupled Eqs. (11) and (12) after the value of ζ_1 has been determined.

5. Discussion of the results

The numerical results illustrate the effect of the variation of the dust parameters on the fluid phase velocities. Figs. 1 and 4 illustrate the effect of the permeability on the horizontal velocity component along the vertical centerline and the boundary lower of the channel respectively. They demonstrate the increase of this velocity component with increasing permeability in the lower region of the channel. In the upper regions, the effect of the sink becomes more noticeable in attracting the fluid faster for lower values of permeability.

Fig. 5 illustrates the effect of the Forchheimer drag coefficient on the fluid-phase horizontal velocity component along the boundary lower of the channel. It demonstrates the decrease in this velocity component with increasing coefficient in the lower regions of the channel.

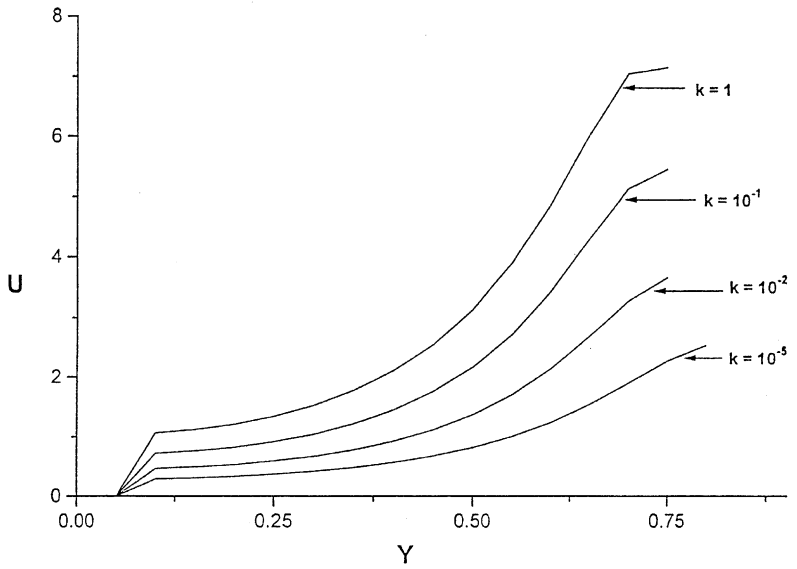

Fig. 1. Horizontal velocity component along the vertical center line of the channel for different permeability and $C_d = 0.5$, $Re = 1$.

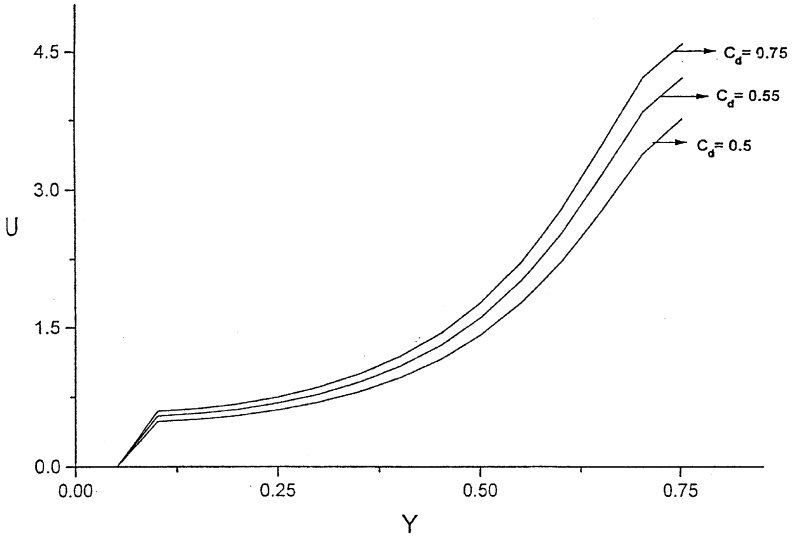

Fig. 2. Horizontal velocity component along the vertical center line of the channel for different Forchheimer drag coefficient and $K = 10^{-2}$, $Re = 1$.

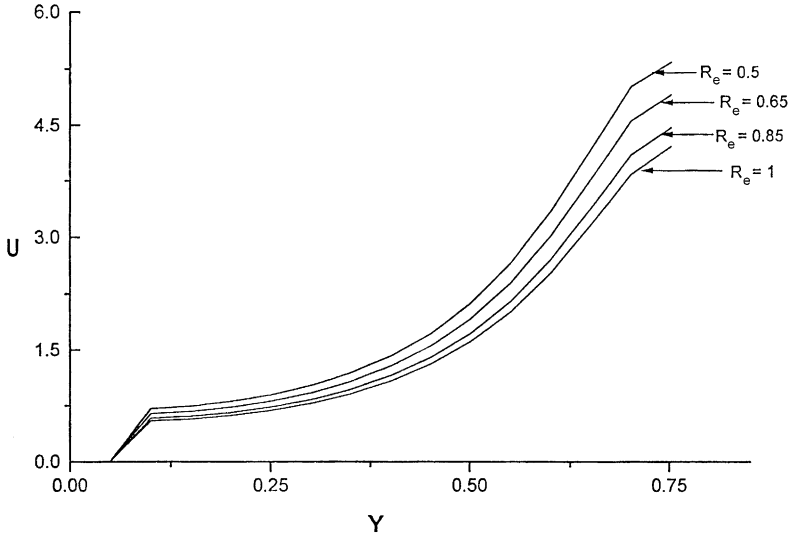

Fig. 3. Horizontal velocity component along the vertical center line of the channel for different Reynolds number and $K = 10^{-2}$, $C_e = 0.75$.

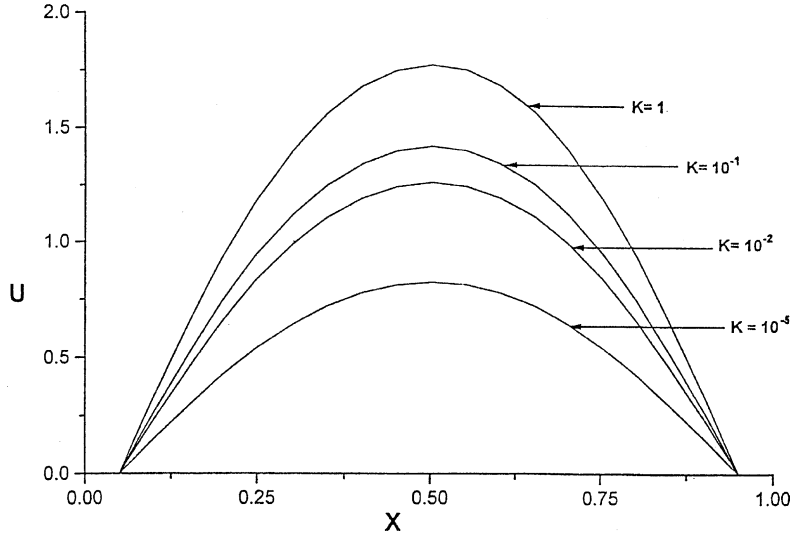

Fig. 4. Horizontal velocity component along the lower boundary of the channel for different permeability and $C_d = 0.75$, $Re = 1$.

Figs. 3 and 6 illustrate the effect of the Reynolds number on the fluid-phase horizontal velocity component along the vertical centerline and the boundary

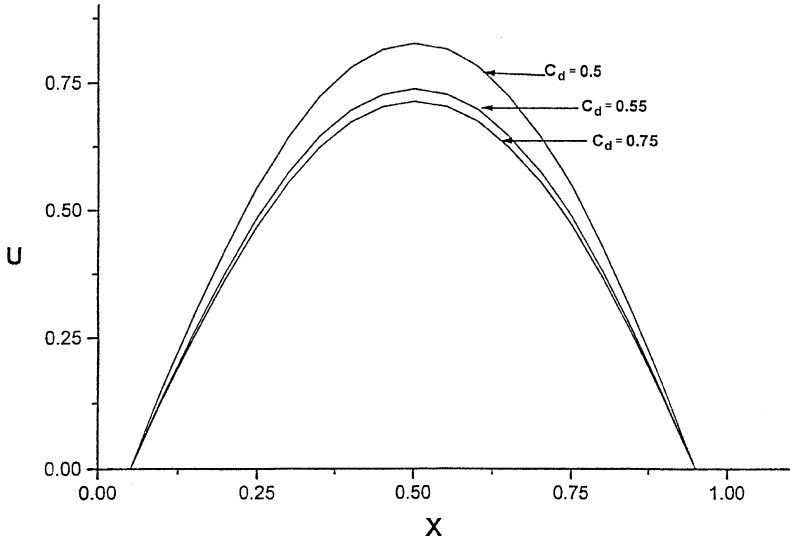

Fig. 5. Horizontal velocity component along the lower boundary of the channel for different Forchheimer drag coefficient and $K = 10^{-2}$, $Re = 1$.

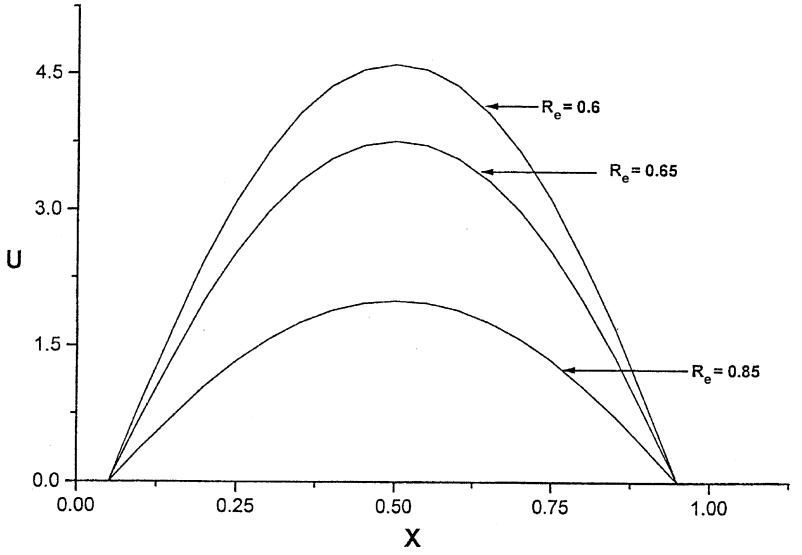

Fig. 6. Horizontal velocity component along the lower boundary of the channel for different Reynolds number and $K = 10^{-2}$, $C_d = 0.75$.

lower of the channel. The demonstrate the decrease in this velocity component with increasing Reynolds number in the lower regions of the channel.

Fig. 7 describes the effect of the permeability on the horizontal velocity component along the horizontal centerline of the channel. It demonstrates the increase of this velocity component with increasing permeability.

Figs. 2 and 8 illustrate the effect of the Forchheimer drag coefficient on the fluid-phase vertical and horizontal velocity component along the vertical and horizontal centerlines of the channel respectively. These results demonstrate the increase in this velocity component with increasing Forchheimer drag coefficient C_d.

Fig. 9 demonstrates the effect of the Reynolds number on the fluid-phase horizontal velocity component along the horizontal centerline of the channel. It demonstrates the decrease in this velocity component with increasing Reynolds number.

The increase of the velocity component in the lower part of the channel, and its decrease in the upper part as C_d increases sheds some light on the appropriate value of C_d. Although a critical value of C_d has not been determined in th is study, the above behavior indicates that the critical value of C_d is approximately.

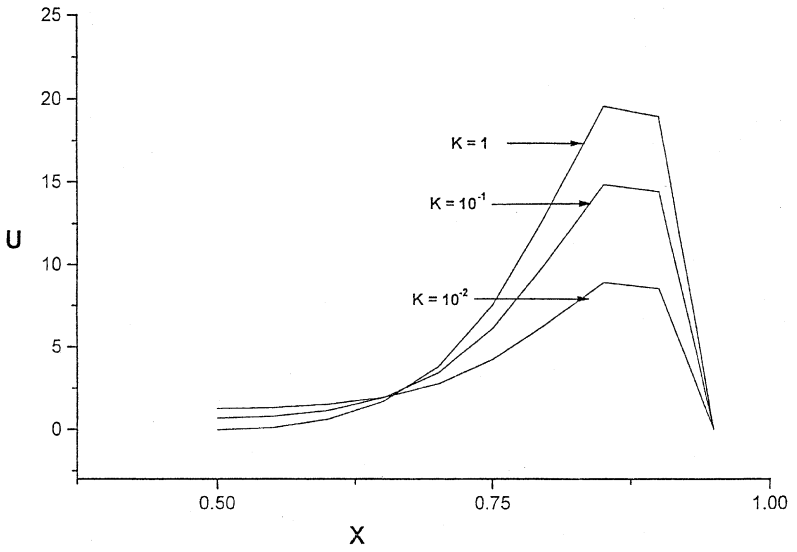

Fig. 7. Horizontal velocity component along the horizontal center line of the channel for different permeability and $C_d = 0.75$, $Re = 1$.

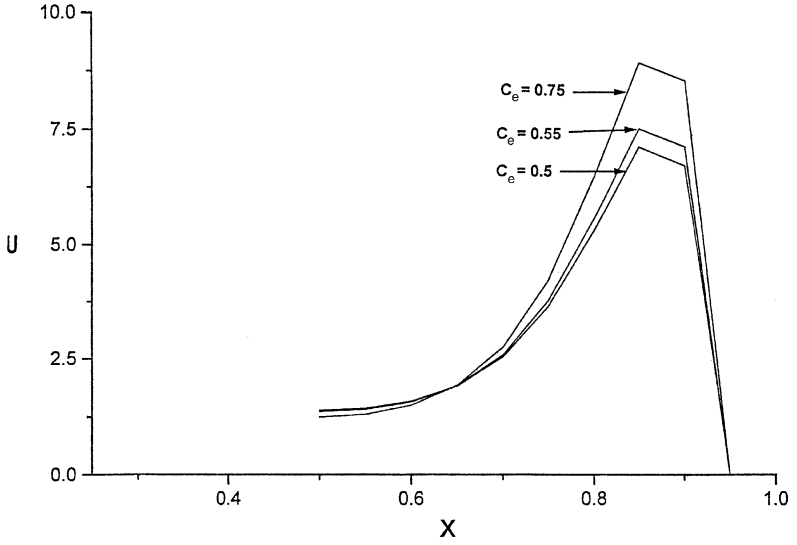

Fig. 8. Horizontal velocity component along the horizontal center line of the channel for different Forchheimer drag coefficient and $K = 10^{-2}$, $Re = 1$.

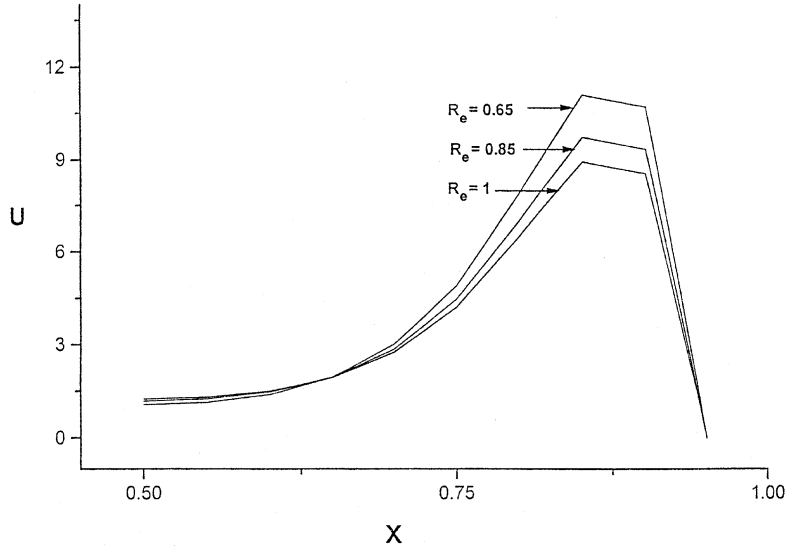

Fig. 9. Horizontal velocity component along the horizontal center line of the channel for different Reynolds number and $K = 10^{-2}$, $C_d = 0.75$.

References

[1] A.J. Chamkha, Analytical solutions for flow of a dusty fluid between two porous flat plates, Trans. ASME, J. Fluids Eng. 116 (1994) 354–356.
[2] C. Chow, An Introduction to Computational Fluid Mechanics, Wiley, New York, 1979.
[3] M.H. Hamdan, R.M. Barren, On the Darcy–Lapwood–Brinkman–Saffman dusty fluid flow models in porous media. Part 1. Models development, J. Appl. Math. Comput. 54 (1) (1993) 65–79.
[4] M.H. Hamdan, R.M. Barron, Gas-particulate through isotropic porous media, Part II. Boundary and entry conditions, in: D.T. Mook, D.L. Zagottis, (Eds.), Proceedings, Third PAN AMERICAN Congress of Applied Mechanics, January 1993, pp. 307–310.
[5] M.H. Hamdan, R.M. Barren, Fluid flow through curved porous channels, Math. Computer Sci. (August) (1990).
[6] M.H. Hamdan, R.M. Barron, A dusty gas flow model in porous media, Comput. Applied Math. 30 (1990) 21–37.
[7] M.H. Hamdan, R.A.R. Ford, Numerical simulation of gas particulate flow through curvilinear porous channels, J. Appl. Math. Comput. 4 (1998) 267–284.
[8] K. Takataka, One-way and two-way interaction gas-particulate flow through porous media, MA thesis, Alquds University, Department of Mathematics, Jerusalem, 2001.
[9] A. Newneier, Introduction to Numerical Analysis, Cambridge University Press, Cambridge, 2001.